AGU PUBLICATIONS

Geophysical Research Letters

RESEARCH LETTER
10.1002/2017GL076336

Key Points:
- Investigation of the ground deformation and source geometry of the 2017 Ischia Island earthquake (Italy) is discussed
- The available seismological, GPS, and DInSAR data permit to investigate the causative fault and define its geometry and kinematics
- The results suggest that the rheology properties of the crust beneath the Ischia Island have an influence on the volcano-tectonic processes

Supporting Information:
- Supporting Information S1
- Data Set S1
- Data Set S2
- Data Set S3
- Data Set S4
- Data Set S5
- Data Set S6
- Data Set S7
- Data Set S8
- Data Set S9
- Data Set S10
- Data Set S11
- Data Set S12
- Data Set S13
- Data Set S14

Correspondence to:
P. Tizzani,
tizzani.p@irea.cnr.it

Citation:
De Novellis, V., Carlino, S., Castaldo, R., Tramelli, A., De Luca, C., Pino, N. A., et al. (2018). The 21 August 2017 Ischia (Italy) earthquake source model inferred from seismological, GPS, and DInSAR measurements. *Geophysical Research Letters*, *45*. https://doi.org/10.1002/2017GL076336

Received 9 NOV 2017
Accepted 5 FEB 2018
Accepted article online 12 FEB 2018

©2018. The Authors.
This is an open access article under the terms of the Creative Commons Attribution-NonCommercial-NoDerivs License, which permits use and distribution in any medium, provided the original work is properly cited, the use is non-commercial and no modifications or adaptations are made.

The 21 August 2017 Ischia (Italy) Earthquake Source Model Inferred From Seismological, GPS, and DInSAR Measurements

V. De Novellis[1], S. Carlino[2], R. Castaldo[1], A. Tramelli[2], C. De Luca[1], N. A. Pino[2], S. Pepe[1], V. Convertito[2], I. Zinno[1], P. De Martino[2], M. Bonano[3], F. Giudicepietro[2], F. Casu[1], G. Macedonio[2], M. Manunta[1], C. Cardaci[4], M. Manzo[1], D. Di Bucci[4], G. Solaro[1], G. Zeni[1], R. Lanari[1], F. Bianco[2], and P. Tizzani[1]

[1]IREA, CNR, Naples, Italy, [2]Osservatorio Vesuviano, Naples, Italy, [3]IMAA, CNR, Potenza, Italy, [4]Dipartimento della Protezione Civile, Rome, Italy

Abstract The causative source of the first damaging earthquake instrumentally recorded in the Island of Ischia, occurred on 21 August 2017, has been studied through a multiparametric geophysical approach. In order to investigate the source geometry and kinematics we exploit seismological, Global Positioning System, and Sentinel-1 and COSMO-SkyMed differential interferometric synthetic aperture radar coseismic measurements. Our results indicate that the retrieved solutions from the geodetic data modeling and the seismological data are plausible; in particular, the best fit solution consists of an E-W striking, south dipping normal fault, with its center located at a depth of 800 m. Moreover, the retrieved causative fault is consistent with the rheological stratification of the crust in this zone. This study allows us to improve the knowledge of the volcano-tectonic processes occurring on the Island, which is crucial for a better assessment of the seismic risk in the area.

1. Introduction

The Ischia earthquake (IE) (M_w 3.9–M_d 4.0; I_{max} EMS 8), occurred on 21 August 2017 (18:57 UTC), struck the northern sector of the active volcanic Ischia Island (Southern Italy) causing two casualties, 42 injuries, and extensive damage to the Casamicciola Terme town and its surroundings, along the northern structural rim of Mount Epomeo (Figure 1a); it was followed by a seismic sequence of almost 20 earthquakes with significantly lower magnitude (Figure S1). Moreover, geological coseismic effects, among which fractures and small rock falls, have been induced over an area of ~2.5 km^2 (Azzaro et al., 2017; EMERGEO Working Group, Nappi et al., 2017).

Seismicity in volcanic areas shows that earthquakes generally have a low magnitude and they do not produce serious damage (McNutt, 2005; Zobin, 2003); however, in a limited number of cases, earthquakes occurring in volcanic areas have been associated to catastrophic effects, thus deserving great attention (Silveira et al., 2003). This is the case of the Ischia Island where low seismic energy events can be associated to high seismic risk. The historical seismic activity of the Ischia Island is recognized since the thirteenth century and caused serious damage, thousands of casualties, and often landslides and surface breaks (Carlino et al., 2010). Macroseismic observations have shown that historical earthquakes are mainly located at Casamicciola Terme, in the northern sector of the Island. These events occurred with short recurrence times, displaying low magnitude (inferred from macroseismic data), and high epicentral intensity, up to 11° MCS, as in the case of the 1883 earthquake (Cubellis & Luongo, 1998). In this case the magnitude (which ranges from 4.2 to 5.2) was inferred from the empirical relationships, for volcanic areas, that correlate this parameter to the maximum intensity, the extension of the source, and the involved area (Cubellis & Luongo, 1998; Okada, 1983; Shebalin, 1972). Macroseismic data also show that earthquakes are characterized by very shallow hypocenter depths (1–2 km), as demonstrated by high-intensity values recorded in the epicentral area and strong attenuation (Carlino et al., 2010). Following the 1883 earthquake, an aseismic period was observed in the Island, but low-magnitude earthquakes have been recorded in the last 40 years in the northern part of the Island (Figure S2).

The most significant seismic activity at Ischia appears to be mainly related to the Mount Epomeo, an upraised structure that dominates the central part of the Island and is interpreted as a resurgent block (volcanic horst)

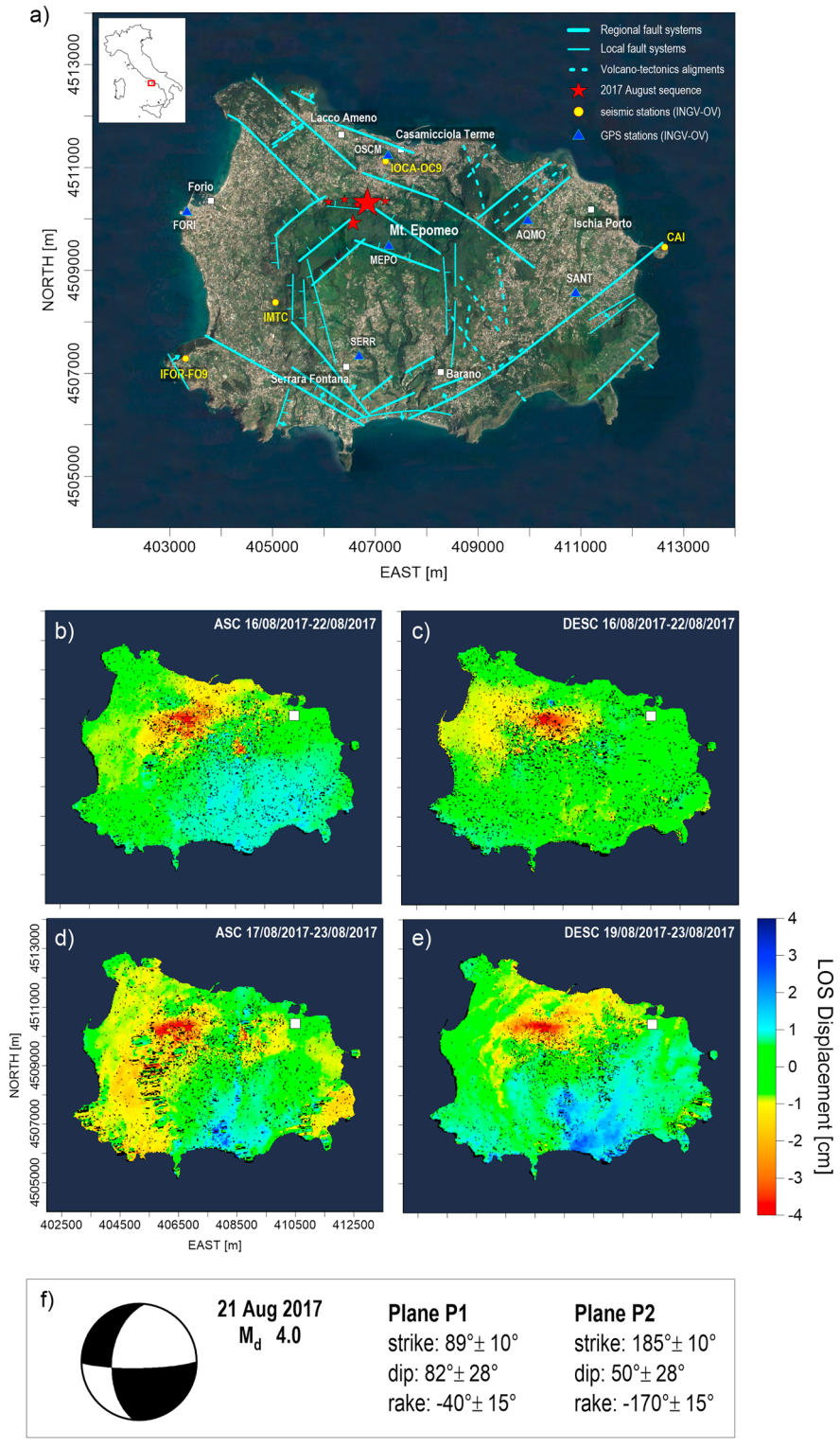

Figure 1. Study area and geodetic measurements. (a) Simplified structural map superimposed on an optical image of the Ischia Island. The structural framework is redrawn from Acocella and Funiciello (1999), where arrows display dipping; hatches on the downthrown side. The biggest red star indicates the location of the 21 August 2017 main shock, while the smaller ones indicate the seismic sequence from 21–30 August 2017; the locations of the seismic and cGPS stations are reported as yellow points and blue triangles, respectively. (b–e) DInSAR (line of sight [LOS]) displacement maps computed by using S1 images acquired from: (b) ascending orbits on 16–22 August 2017, (c) descending orbits on 16–22 August 2017, (d) ascending orbits on 17–23 August 2017, and (e) CSK images acquired from descending orbits on 19–23 August 2017. The white square in panels (b-e) represents the DInSAR reference pixel. (f) Focal mechanism and the P1 and P2 fault plane solution parameters.

that, from at least 33 ka to about 5 ka, rose of about 800 m (Vezzoli, 1988), possibly due to the magma pushing (Carlino, 2012). The edges of Mount Epomeo are marked by a system of subvertical faults, with NW-SE, NE-SW, N-S, and E-W strike (Sbrana et al., 2009; Tibaldi & Vezzoli, 1998). The northern part of the block, dislocated by roughly E-W and SW-NE faults, is the source area of the historical seismicity.

Since Roman time an inversion of the resurgence seems to be occurred at least in the northern sector of the Island (Buchner, 1986), as also recently recorded by Global Positioning System (GPS) data, leveling surveys, and differential interferometric synthetic aperture radar (DInSAR) measurements, showing a general trend of slow subsidence with the maximum values of about 1 cm/year (De Martino et al., 2011; Manzo et al., 2006).

In this study, we take advantage of the available seismological, GPS, and DInSAR measurements to investigate the causative seismogenic fault of the IE main shock and to define its geometry and kinematics. In particular, we jointly exploit three Sentinel-1 (S1) and one COSMO-SkyMed (CSK) displacement maps, obtained from ascending and descending orbits, and the available GPS measurements to model the finite fault in an elastic and homogeneous half-space. Subsequently, we benefit of the seismological data to support our findings relevant to the modeled source.

Our results allow us to improve the knowledge of the volcano-tectonic processes occurring on the Island, which is crucial for a better assessment of the seismic risk.

2. Exploited Data

In order to investigate the source responsible for the main shock of the 2017 seismic sequence that affected the Casamicciola Terme area, we analyze the seismological data, DInSAR, and GPS measurements discussed in the following.

2.1. DInSAR and GPS Measurements

The ground displacements caused by the earthquake have been detected through DInSAR and GPS measurements. Regarding the DInSAR data, we generate several ascending and descending coseismic interferograms by exploiting both S1 and CSK SAR data. Among them, we select four interferometric pairs (three from S1 data and one from CSK ones) showing better interferometric coherence characteristics. Accordingly, the maximum temporal baseline is of 6 days for the selected S1 interferograms (Figures 1b–1d) and 4 days for the CSK one (Figure 1e); more detailed characteristics are reported in Figure S3. Before generating the S1 interferograms, we coregister the SLC images by using the enhanced spectral diversity approach (Yague-Martinez et al., 2016). Moreover, following the interferograms generation, we first unwrap the interferograms relevant to the selected interferometric SAR data pairs by applying a minimum-cost flow approach (Pepe & Lanari, 2006); subsequently, we compensate for possible atmospheric phase artifacts correlated with the topography of the area to finally retrieve the line of sight displacement maps presented in Figures 1b–1e. Note also that all the measurements are referred to a reference pixel located at Ischia Porto.

In spite of some spatially random signals due to residual atmospheric phase delays (Hanssen, 2001), all the generated displacement maps present a consistent range increase pattern localized in an area south of Casamicciola Terme, independently from the orbit pass, look angle, and interferometric pair (see Figures 1b–1e and S3). This implies that the detected displacements are mainly vertical (i.e., subsidence; see also Figure S4) (Manzo et al., 2006). The maximum range change is of about 4 cm in line of sight. The shape of the displacement pattern shows an E-W alignment, which is in good agreement with the aftershock epicenter distribution (Figure 1a). The extension of the deforming area is of about 1 km^2.

For what concerns the GPS measurements, six continuous GPS (cGPS) stations managed by the Istituto Nazionale di Geofisica e Vulcanologia (INGV) Osservatorio Vesuviano are operating at Ischia Island (Figure 1a). Their data processing has been performed by using the Bernese GPS software 5.0 (Dach et al., 2007); a full description of the processing strategies is reported in De Martino et al. (2014). Following the main shock seismic event, some cGPS stations experienced a coseismic deformation. These displacements have been obtained by estimating offsets in the position time-series by considering the time interval extending from 15 days before and 5 days after the main shock, respectively. In particular, the cGPS station on Mount Epomeo (MEPO) shows a maximum horizontal displacement of about 1.5 cm in NNW

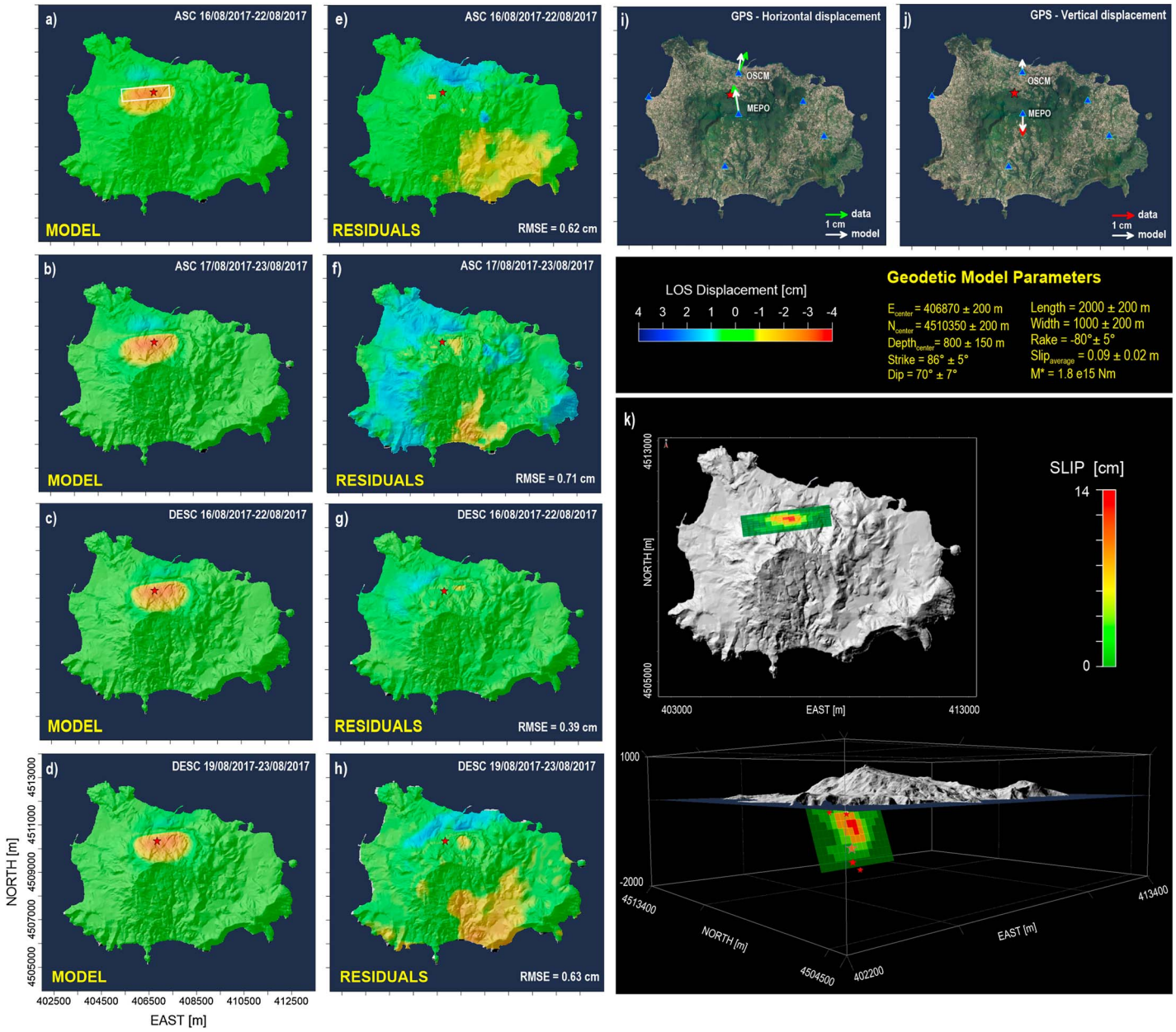

Figure 2. Source modeling results. Line of sight (LOS) projected displacement maps computed from the retrieved analytical model for the following interferograms: (a) 16–22 August 2017 (S1), (b) 17–23 August 2017 (S1), (c) 16–22 August 2017 (S1), and (d) 19–23 August 2017 (CSK). Their corresponding residual maps are shown in (e–h), respectively. (i) Observed (green) and predicted (white) cGPS horizontal displacements relevant to the stations OSCM, MEPO, and SERR; (j) observed (red) and predicted (white) cGPS vertical displacements. The retrieved model parameters are also reported as well as (k) the distributed slip over a mesh of 200 × 200 m^2 displayed in map view and 3D view, respectively. The red stars indicate the 2017 main event and the aftershocks.

direction, whereas the one located in Casamicciola Terme (OSCM) moved of about 1.0 cm toward NNE. Only the cGPS MEPO station seems to be affected by a vertical coseismic displacement with a subsidence of about 1.0 cm (Figures 2i–2j).

2.2. Seismological Data

The IE M_w 3.9 (M_d 4.0) was recorded by the INGV seismic stations up to 40 km away from the event area and nucleated at a depth of about 1.2 (±0.2) km on the northern rim of the Mount Epomeo block. The aftershocks were instead detected only by the seismic stations located on the Island (Figure S1). In particular, most of

them were only recorded in the Casamicciola Terme Observatory site, where the IOCA and OC9 sensors are located (see Figure 1a). All the earthquakes with, at least, four phase pickings (the main event and five aftershocks) were located by using the NonLinLoc code (Lomax et al., 2000) and an unified 3D velocity model for the Neapolitan volcanic areas, extending from the Ischia Island to the Apennine Mountains (D'Auria et al., 2008). This model has been obtained through a weighted average of the local tomographic velocity models selected from the existing literature (Improta et al., 2000; Judenherc & Zollo, 2004; Scarpa et al., 2002; Vanorio et al., 2005; Zollo et al., 2003). By using this model we account for the velocity differences between the Campi Flegrei caldera and the Ischia Island structures, being this area characterized by high contrast in the elastic properties, particularly at the Campi Flegrei caldera boundaries (Tramelli et al., 2006). The most accurate earthquake locations are reported in Figures 1a and S2 with the epicenters distribution showing an E-W preferential direction. We compute the focal mechanism for the main event (Figure 1f) by using only the *P* wave polarities at 11 stations (Figure S2) of the seismic network of Ischia, Campi Flegrei, and the regional network, characterized by a clearly detectable signal, and by applying the FPFIT code (Reasenberg & Oppenheimer, 1985). In Figure 1f we also present the achieved focal mechanism and the retrieved fault plane parameters. We further remark that although the estimated rake indicates a transcurrent component in the focal mechanism, the available *P* wave polarities do not allow to well constrain this parameter.

3. Modeling

3.1. Geodetic Modeling

In order to investigate the seismogenic source parameters we jointly invert the selected DInSAR coseismic displacement maps and the GPS measurements. Note that the DInSAR measurements have been resampled on a regular grid with a mesh of 100×100 m^2. Moreover, we also apply a low-pass filter to each DInSAR displacement map in order to mitigate the decorrelation effects (Franceschetti & Lanari, 1999); note also that the SAR pixels characterized by very high decorrelation effects (i.e., with very low interferometric coherence) have been excluded from our analysis.

Our modeling strategy follows a well-established two-step approach: a nonlinear inversion to estimate the fault plane parameters, followed by a linear inversion to retrieve the slip distribution on the fault plane (Atzori et al., 2009; Solaro et al., 2016). Accordingly, the displacement maps are first modeled through a fault plane and its parameters are retrieved by using a nonlinear inversion based on the Levenberg-Marquardt least squares approach (Marquardt, 1963). The choice of using a single planar source in the optimization procedure is conditioned by the presence of one distinctive lobe in the detected ground deformation pattern (Figures 1b–1e). Specifically, we investigate a finite dislocation planar source in an elastic and homogeneous half-space (Okada, 1985), for which all source parameters are set free during the inversion. We find that the best fit solution consists of an E-W striking south dipping normal fault with its center located at a depth of 800 m; the retrieved best fit parameters are reported in Figure 2. The residual patterns (i.e., the difference between measured and modeled displacements) and the RMSE values for each interferogram are also reported in Figures 2b, 2d, 2f, and 2h; note that the higher residuals are associated to residual atmospheric artifacts. In addition, we perform a statistical analysis on the retrieved fault parameters (Figure S5). The model solution is also compared with the horizontal (Figure 2i) and the vertical (Figure 2j) GPS components highlighting a good agreement also for these measurements.

In order to have a more accurate estimate of the slip along the fault plane, a distributed slip pattern is computed by partitioning the plane into 15×9 patches each of these extending for about 200×200 m^2. Also, in this case, we jointly invert the selected ascending and descending interferograms and GPS measurements. To this aim, a linear inversion procedure has been performed by starting from the parameters of the previous nonlinear inversion and searching for the differential slip on each patch (Atzori et al., 2008). Note also that the fault length and width are extended to consider the border effects as negligible. We find that the causative fault is characterized by a main region with a maximum slip of about 14 cm at a depth in the 0.7–1.0 km range, along the seismogenic plane (Figure 2k). Finally, we compute a geodetic moment (M*) of about 1.8×10^{15} Nm, corresponding to a moment magnitude of about M_w 4.1.

3.2. Seismic Waveform Analysis and Modeling

We analyze the seismic waveforms recorded by the accelerometer (Episensor ES-T) installed at the Casamicciola Terme Observatory (IOCA), at about 1 km distance from the epicenter (Figure 1a). In

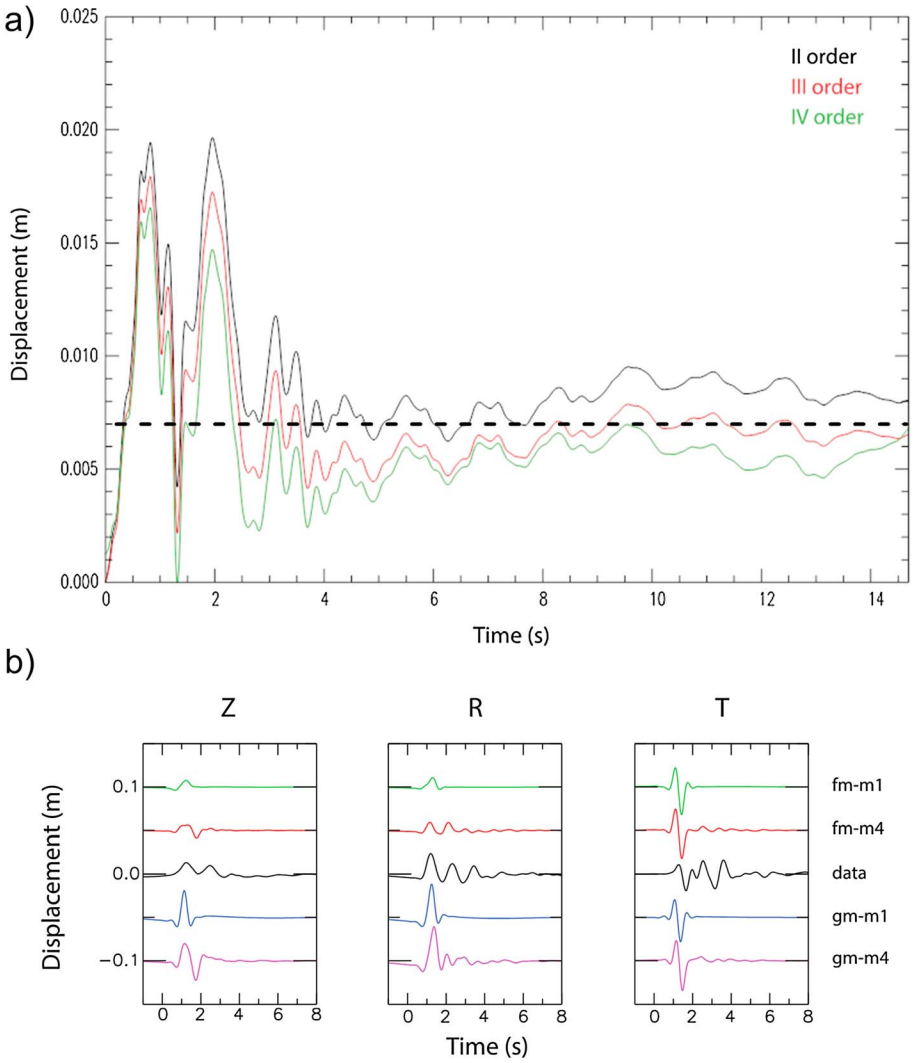

Figure 3. Seismic waveforms analysis and their modeling. (a) Coseismic vertical displacements retrieved from the acceleration measurements recorded at the IOCA station (see Figure 1a). Each line represents the result obtained by removing a polynomial function of the indicated order. (b) Comparison between the observed displacements (obtained from double integration of the recorder acceleration) at IOCA and the synthetic ones computed for the focal mechanism derived from the first motion (fm) polarities and the geodetic modeling (gm), respectively. A homogeneous half plane (m1) and a four-layered structural model (m4) have been used. The waveforms are rotated to the vertical (Z), radial (R), and transversal (T) components and band-pass filtered between 0.1 Hz and 2.0 Hz.

particular, in order to investigate the coseismic permanent vertical motion, we compute the vertical displacement waveform by exploiting the recorded acceleration. Note that retrieving static vertical displacement from seismic waveforms is a rather delicate operation requiring careful analysis, but it can provide robust results (Pino & Di Luccio, 2005, 2009). The main problems usually relate either to the long-period drift introduced by the needed double integration (for accelerograms) (Boore, 2001) or to the removal of the instrument response (Zhu, 2003). Several methods have been proposed to correct for the above mentioned drift; here we follow the scheme proposed by Zhu (2003), removing the drift from the displacement waveforms by using polynomial functions. The Figure 3a shows the final vertical displacement obtained for second-, third-, and fourth-order polynomials. All the resulting waveforms show a vertical uplift of about 0.7 cm. Note that although this value resulting from the waveform analysis is below the resolution of the GPS vertical component, it is in a good agreement with the vertical component of the modeled displacement retrieved from the geodetic data inversion (Figures S4c and S4d).

In order to further constrain the retrieved fault parameters, we perform an additional analysis on the seismic waveforms. More specifically, we compare the observed waveforms at IOCA with the synthetic seismograms computed for the two source models relevant to the retrieved focal mechanism for plane P1 (Figure 1f) and to the geodetic model (Figure 2); these seismograms are obtained by means of a reflectivity based method (Giardini et al., 1995) with a point-source and double-couple mechanism, and considering two distinct structural models: a homogeneous half space (V_P = 2.5 km/s; V_S = 1.4 km/s) and a four-layered, laterally homogeneous structure (Figure 3b and Table S1). Note that for the geodetic model, the source is located at the fault center, whereas for the polarity-derived mechanism the source is located at the hypocenter, being the latter deeper than the fault center. For both models, we used the seismic moment $M_0 = 1.0 \times 10^{15}$ Nm.

The comparative analysis between the measured and the modeled waveforms, shown in Figure 3b, indicates that for the synthetic seismograms (referred to as synthetics) both sources provide a reasonable fit with the recorded waveforms (Table S2). We observe that the first pulse duration, controlled by the *S-P* arrival time, is in better agreement with the longer source-to-station paths, that is, with the deeper hypocentral location of the first motion polarity source and with the longer paths of the four-layered model. This latter produces minor oscillations in the synthetics that slightly increase the misfit. We also remark that the observed relative maximum amplitude of the three components is more compatible with a higher rake angle (i.e., with the geodetic model), as evident if the misfit for each model is computed with the synthetics rescaled by equating the maximum amplitude of the vertical component to the observed one (Table S3).

Overall, the waveform analysis points out that independently of the adopted structural model, the seismogenic fault responsible for the IE is characterized by (i) a E-W striking fault; (ii) a south dipping, high-angle plane; and (iii) a rake value showing a low-to-null strike-slip component.

4. Discussions and Conclusion

The 21 August 2017 IE represents the largest seismic event affecting the Island ever observed with modern techniques. The level of damage and its distribution (EMERGEO Working Group, Nappi et al., 2017; Gruppo di Lavoro INGV sul terremoto dell'isola di Ischia, 2017), with respect to the magnitude, agree with the historical observations of low magnitude-high intensity occurrence and strong attenuation (Carlino et al., 2010). The most relevant damage, observed just in a narrow area of Casamicciola Terme, is related to the shallowness of the source.

A multidisciplinary approach allowed us to investigate the causative source of the IE event. In particular, we have exploited seismological data, multisensor/multiorbit DInSAR measurements, and cGPS ones (Figure 1) to investigate the seismogenic source through analytical modeling techniques.

The joint inversion of the DInSAR and cGPS coseismic measurements allows us to estimate the fault plane parameters and to retrieve the associated slip distribution. We find a main patch of slip (with values up to 14 cm) located at the center of the fault plane at a depth of 800 m (Figure 2). This result provides a picture of the seismogenic mechanism of the earthquake, dominated by a normal fault mechanism where the hanging block (located in the northern part of Mount Epomeo) moves downward. In particular, the retrieved seismogenic fault responsible for the IE is characterized by (i) a E-W striking fault (86°); (ii) a south dipping, high-angle plane (70°); and (iii) a rake value close to −90°. These findings are in rather good agreement with the recorded aftershock alignment along the E-W direction and with the computed focal mechanism relevant to the plane P1 (Figure 1f), thus allowing to resolve for the nonuniqueness of the fault plane solutions. The only main difference between the focal plane P1 and the geodetic modeling solution is relevant to the rake values that, for the former case, results to be −40°±15°. However, although this rake estimate indicates a transcurrent component in the focal mechanism, its value is not well constrained by the *P* wave polarities available for this earthquake. Moreover, the seismic waveforms at IOCA station show a vertical uplift of about 0.7 cm, which is in good agreement with the modeled displacements.

Two seismic waveform forward modeling have been also carried out by considering the focal mechanism and the geodetic modeling results, respectively. Both models confirm that a high-angle normal fault, with low-to-null transcurrent component, is required in order to satisfactorily reproduce the observed transient ground motion (Figure 3). In this case the main difference with respect to the geodetic modeling results is related to the retrieved seismic moment, which is 1.0×10^{15} Nm. The discrepancy between the geodetic

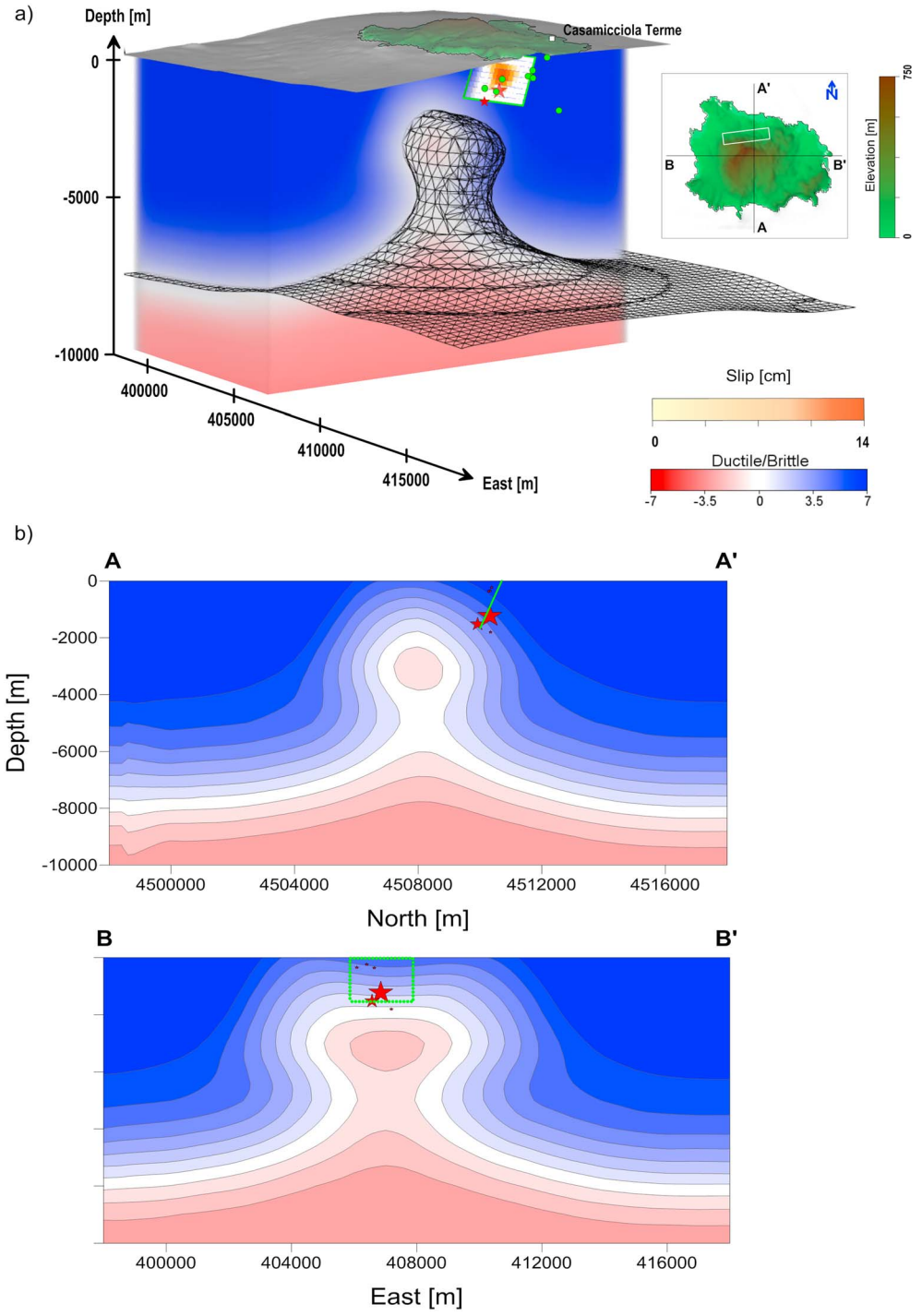

Figure 4. Source modeling results in the rheological scenario. (a) 3D prospective view of the rheological stratification of the crust beneath Ischia Island. The grey wireframe isosurface represents the brittle/ductile transition from Castaldo et al. (2017). The retrieved fault plane (see Figure 2k) and the distributed slip are also reported. The locations of the selected AA′ and BB′ cross sections, investigated in the following, are displayed in the upper left corner. The red stars and the green dots indicate the location of the seismicity recorded during August 2017 and during the time interval 1999–2013, respectively. (b) Selected cross sections shown in (a) with the contour map of the computed rheological stratification of the crust; the retrieved fault plane is reported with the continuous green line in AA′ and the dotted one (projected) in BB′.

($M^* = 1.8 \times 10^{15}$ Nm) and the seismic moment estimations can be attributed to a number of factors such as a possible small component of deformation aseismically accommodated. Note also that according to the classification proposed by Wassermann (2002), the frequency analysis of recorded seismic waveforms allows us to classify the IE as shallow volcanic-tectonic event (above about 1–2 km).

We further remark that the 2017 seismic sequence occurs in the same area where the previous seismicity of Ischia Island was located (Rovida et al., 2016) (Figures 4 and S2). The E-W distribution of the seismic sequence spreads along the main system of faults arranged in parallel segments (Acocella & Funiciello, 1999) over an area, whose dimension is compatible with the fault length inferred from our inversion results. The subvertical normal fault of the earthquake with a southward dipping is in good agreement with the structural framework of Mount Epomeo proposed in the available literature (Acocella et al., 2001; Acocella & Funiciello, 1999; Molin et al., 2003) and with no field evidences of reverse fault systems (Marotta & De Vita, 2014). Moreover, the bathymetric surveys performed in the surrounding region of the volcanic Island do not reveal the existence of morphological elements that could be associated with compressional fault structures (Aiello et al., 2009).

Our study confirms that the seismicity of the northern side of the Island is associated to a local seismogenic structure that is stressed, and periodically reactivated, by the loading of the Mount Epomeo along its maximum elevation sector (Carlino et al., 2014). In this context, the retrieved normal fault mechanism is very likely induced by the observed long-term subsidence phase (Manzo et al., 2006), since the lithostatic load represents the principal vertical stress. The comparison between the rheological model proposed by Castaldo et al. (2017) and the seismicity recorded at Ischia Island clearly shows that the earthquake hypocenters are at shallower depth than brittle/ductile transition (at about 2 km depth beneath Mount Epomeo) (Figure 4a). This finding is particularly evident if we superimpose the retrieved fault model on the rheological stratification of the area (Figure 4b). Accordingly, our results suggest that (i) the seismicity of Ischia is not associated to magma injection and (ii) the rheology properties of the crust beneath the Ischia Island have an influence on the ongoing volcano-tectonic processes.

Acknowledgments
This work has been supported in the framework of the DPC-IREA Agreement and DPC-INGV Agreement 2012–2021. The contents of this paper represent the authors' ideas and do not necessarily correspond to the official opinion and policies of the Italian Department of Civil Protection. The work has been also supported by the EPOS-IP project of the European Commission's Horizon 2020 research and innovation programme under grant agreement 676564, the ESA GEP project, the I-AMICA project (Infrastructure of High Technology for Environmental and Climate Monitoring-PONa3_00363), the VULCAMED project (PONa3_00278), and CNR project "Development and application of geophysical method based on the use of remote sensing data" (DTA.AD004.065) —subproject "Modeling of Geophysical processes" (DTA.AD004.065.001). Sentinel-1 data have been provided through the Copernicus Program of the European Union; the COSMO-SkyMed data have been supplied by the Italian Space Agency (ASI), and they have been acquired through a dedicated acquisition plan. The DEM of the investigated zone was acquired through the SRTM archive. We thank the INGV-OV staff involved in the management and maintenance of the seismic and GPS networks and Simone Guarino, Ferdinando Parisi, and Maria Consiglia Rasulo of IREA for their technical support.

References

Acocella, V., & Funiciello, R. (1999). The interaction between regional and local tectonics during resurgent doming: The case of the island of Ischia, Italy. *Journal of Volcanology and Geothermal Research*, *88*(1-2), 109–123. https://doi.org/10.1016/S0377-0273(98)00109-7

Acocella, V., Cifelli, F., & Funiciello, R. (2001). The control of overburden thickness on resurgent domes: Insights from analogue models. *Journal of Volcanology and Geothermal Research*, *111*(1-4), 137–153. https://doi.org/10.1016/S0377-0273(01)00224-4

Aiello, G., Marsella, E., & Passaro, S. (2009). Submarine instability processes on the continental slopes off the Campania Region (southern Tyrrhenian Sea, Italy): The case history of Ischia Island (Naples Bay). *Bollettino di Geofisica Teorica ed Applicata*, *50*(2), 193–207.

Atzori, S., Manunta, M., Fornaro, G., Ganas, A., & Salvi, S. (2008). Postseismic displacement of the 1999 Athens earthquake retrieved by the differential interferometry by synthetic aperture radar time series. *Journal of Geophysical Research*, *113*, B09309. https://doi.org/10.1029/2007JB005504

Atzori, S., Hunstad, I., Chini, M., Salvi, S., Tolomei, C., Bignami, C., et al. (2009). Finite fault inversionof DInSAR coseismic displacement of the 2009 L'Aquila earthquake (central Italy). *Geophysical Research Letters*, *36*, L15305. https://doi.org/10.1029/2009GL039293

Azzaro, R., Del Mese, S., Martini, G., Paolini, S., Screpanti, A., Verrubbi, V., & Tertulliani, A. (2017). QUEST, Rilievo macrosismico per il terremoto dell'isola di Ischia del 21agosto 2017. *Rapporto interno*, 1–6. https://doi.org/10.5281/zenodo.849091

Boore, D. M. (2001). Effect of baseline corrections on displacements and response spectra for several recordings of the 1999 Chi-Chi, Taiwan, earthquake. *Bulletin of the Seismological Society of America*, *91*(5), 1199–1211. https://doi.org/10.1785/0120000703

Buchner, G. (1986). Eruzioni vulcaniche e fenomeni vulcano-tettonici di eta` preistorica e storica nell'isola d'Ischia. In A. Livadie (Ed.), *Tremblements de terre, éruptions volcaniques et vie des hommes dans la*. Campanie antique. Napoli (pp. 145–188).

Carlino, S. (2012). The process of resurgence for Ischia Island (southern Italy) since 55 ka: The laccolith model and implications for eruption forecasting. *Bulletin of Volcanology*, *74*(5), 947–961. https://doi.org/10.1007/s00445-012-0578-0

Carlino, S., Cubellis, E., & Marturano, A. (2010). The catastrophic 1883 earthquake at the island of Ischia (southern Italy): macroseismic data and the role of geological conditions. *Natural Hazards*, *52*, 231. https://doi.org/10.1007/s11069-009-9367-2

Carlino, S., Somma, R., Troiano, A., Di Giuseppe, M. G., Troise, C., & De Natale, G. (2014). The geothermal system of Ischia Island (southern Italy): Critical review and sustainability analysis of geothermal resource for electricity generation. *Renewable Energy*, *62*, 177–196. https://doi.org/10.1016/j.renene.2013.06.052

Castaldo, R., Gola, G., Santilano, A., De Novellis, V., Pepe, S., Manzo, M., & Tizzani, P. (2017). The role of thermo-rheological properties of the crust beneath Ischia Island (Southern Italy) in the modulation of the ground deformation pattern. *Journal of Volcanology and Geothermal Research*, *344*, 154–173. https://doi.org/10.1016/j.jvolgeores

Cubellis, E., & Luongo, G. (1998). Il terremoto del 28 luglio 1883 a Casamicciola nell'isola d'Ischia – "Il contesto fisico". Monografia N.1 – Servizio Sismico Nazionale (pp. 49–123.). Istituto Poligrafico e Zecca dello Stato, Rome.

Dach, R., Hugentobler, U., Fridez, P., & Meindl, M. (2007). *User manual of the Bernese GPS software 5.0*. Bern, Switzerland: Astron. Inst., Univ. of Bern.

D'Auria, L., Martini, M., Esposito, A., Ricciolino, P., & Giudicepietro, F. (2008). A unified 3D velocity model for the Neapolitan volcanic areas. In W. Marzocchi & A. Zollo (Eds.), *Conception, verification and application of innovative techniques to study active volcanoes* (pp. 375–390). Roma: Istituto Nazionale di Geofisica e Vulcanologia.

De Martino, P., Tammaro, U., Obrizzo, F., Sepe, V., Brandi, G., D'Alessandro, A., et al. (2011). Quaderni di Geofisica (No. 95).

De Martino, P., Tammaro, U., & Obrizzo, F. (2014). GPS time series at Campi Flegrei Caldera (2000 - 2013). *Annals of Geophysics*, *57*(2), S0213. https://doi.org/10.4401/ag-6431S0213

EMERGEO Working Group, Nappi R, et al. (2017). Il terremoto dell'isola di Ischia (Casamicciola) del 21 agosto 2017: Effetti Cosismici. https://doi.org/10.5281/zenodo.1003175

Franceschetti, G., & Lanari, R. (Eds) (1999). *Synthetic aperture radar processing*. New York: CRC Press.

Giardini, D., Palombo, B., & Pino, N. A. (1995). Long-period modelling of MedNet waveforms for the December 13, 1990 eastern Sicily earthquake. *Annali di Geofisica*, *XXXVIII*, 267–282.

Gruppo di Lavoro INGV sul terremoto dell'isola di Ischia (2017). Rapporto di sintesi preliminare sul Terremoto dell'isola d'Ischia (Casamicciola) M4.0 del 21 agosto 2017 (6 settembre 2017). https://doi.org/10.5281/zenodo.886045

Hanssen, R. F. (2001). *Radar interferometry: Data interpretation and error analysis*. Netherlands: Springer Science & Business Media. https://doi.org/10.1007/0-306-47633-9

Improta, L., Iannaccone, G., Capuano, P., Zollo, A., & Scandone, P. (2000). Inferences on the up- per crustal structure of Southern Apennines (Italy) from seismic refraction investigations and subsurface data. *Tectonophysics*, *317*(3-4), 273–298. https://doi.org/10.1016/S0040-1951(99)00267-X

Judenherc, S., & Zollo, A. (2004). The bay of Naples (Southern Italy): Constraints on the volcanic structures inferred from a dense seismic survey. *Journal of Geophysical Research*, *109*, B10312. https://doi.org/10.1029/2003JB002876

Lomax, A., Virieux, J., Volant, P., & Berge, C. (2000). Probabilistic earthquake location in 3D and layered models: Introduction of a Metropolis-Gibbs method and comparison with linear locations. In C. H. Thurber & N. Rabinowitz (Eds.), *Advances in seismic event location*, (pp. 101–134). Amsterdam: Kluwer. https://doi.org/10.1007/978-94-015-9536-0_5

Manzo, M., Ricciardi, G. P., Casu, F., Ventura, G., Zeni, G., Borgström, S., & Lanari, R. (2006). Surface deformation analysis in the Ischia Island (Italy) based on spaceborne radar interferometry. *Journal of Volcanology and Geothermal Research*, *151*(4), 399–416. https://doi.org/10.1016/j.jvolgeores.2005.09.010

Marotta, E., & de Vita, S. (2014). The role of pre-existing tectonic structures and magma chamber shape on the geometry of resurgent blocks: Analogue models. *Journal of Volcanology and Geothermal Research*, *272*, 23–38. https://doi.org/10.1016/j.jvolgeores.2013.12.005

Marquardt, D. (1963). An algorithm for least-squares estimation of nonlinear parameters. *SIAM Journal on Applied Mathematics*, *11*(2), 431–441. https://doi.org/10.1137/0111030

McNutt, S. R. (2005). Volcanic seismology. *Annual Review of Earth and Planetary Sciences*, *32*, 461–491.

Molin, P., Acocella, V., & Funiciello, R. (2003). Structural, seismic and hydrothermal features at the border of an active intermittent resurgent block: Ischia Island (Italy). *Journal of Volcanology and Geothermal Research*, *121*(1-2), 65–81. https://doi.org/10.1016/S0377-0273(02)00412-2

Okada, H. (1983). Comparative study of the earthquake swarms associated to major volcanic activity. In D. Shimozuru & I. Yokoyama (Eds.), *Arc Volcanism: Physics and Tectonics*. (pp 43–61). Tokyo: Terra Scientific Publishing Company.

Okada, Y. (1985). Surface deformation due to shear and tensile faults in a half-space. *Bulletin of the Seismological Society of America*, *75*, 1135–1154.

Pepe, A., & Lanari, R. (2006). On the extension of the minimum cost flow algorithm for phase unwrapping of multitemporal differential SAR interferograms. *IEEE Transactions on Geoscience and Remote Sensing*, *44*(9), 2374–2383. https://doi.org/10.1109/TGRS.2006.873207

Pino, N. A., & Di Luccio, F. (2005). Seismic recording of small zero frequency displacement from moderate events. *Geophysical Research Letters*, *32*, L12304. https://doi.org/10.1029/2005GL022780

Pino, N. A., & Di Luccio, F. (2009). Source complexity of the 6 April 2009 L'Aquila (central Italy) earthquake and its strongest aftershock revealed by elementary seismological analysis. *Geophysical Research Letters*, *36*, L23305. https://doi.org/10.1029/2009GL041331

Reasenberg, P. A., & Oppenheimer, D. (1985). FPFIT, FPPLOT, and FPPAGE: Fortran computer programs for calculating and displaying earthquake fault-plane solutions, U.S. Geological Survey Open-File Report 85–739.

Rovida, A., Locati, M., Camassi, R., Lolli, B., &Gasperini, P. (2016). CPTI15, the 2015 version of the Parametric Catalogue of Italian Earthquakes. https://doi.org/10.6092/INGV.IT-CPTI15

Sbrana, A., Fulignati, P., Marianelli, P., Boyce, A. J., & Cecchetti, A. (2009). Exhumation of an active magmatic–hydrothermal system in a resurgent caldera environment: The example of Ischia (Italy). *Journal of the Geological Society*, *166*(6), 1061–1073. https://doi.org/10.1144/0016-76492009-030

Scarpa, R., Tronca, F., Bianco, F., & Del Pezzo, E. (2002). High resolution velocity structure beneath Mount Vesuvius from seismic array data. *Geophysical Research Letters*, *29*(21), 2040. https://doi.org/10.1029/2002GL015576

Shebalin, N. V. (1972). Macroseismic data as information on source parameters of large earthquake. *Physics of the Earth and Planetary Interiors*, *6*, 316–323.

Silveira, D., Gaspar, J. L., Ferreira, T., & Queiroz, G. (2003). Reassessment of the historical seismic activity with major impact on S. Miguel Island (Azores). *Natural Hazards*, *3*, 1–8.

Solaro, G., De Novellis, V., Castaldo, R., De Luca, C., Lanari, R., Manunta, M., & Casu, F. (2016). Coseismic fault model of Mw 8.3 2015 Illapel earthquake (Chile) retrieved from multi-orbit Sentinel1-A DInSAR measurements. *Remote Sensing*, *8*(4), 323. https://doi.org/10.3390/rs8040323

Tibaldi, A., & Vezzoli, L. (1998). The space problem of caldera resurgence: An example from Ischia Island, Italy. *Geologische Rundschau*, *87*(1), 53–66. https://doi.org/10.1007/s005310050189

Tramelli, A., Del Pezzo, E., Bianco, F., & Boschi, E. (2006). 3D scattering image of the Campi Flegrei caldera (Southern Italy): New hints on the position of the old caldera rim. *Physics of the Earth and Planetary Interiors*, *155*(3-4), 269–280. https://doi.org/10.1016/j.pepi.2005.12.009

Vanorio, T., Virieux, J., Capuano, P., & Russo, G. (2005). Threedimensional seismic tomography from p wave and s wave microearthquake travel times and rock physics characterization of the Campi Flegrei caldera. *Journal of Geophysical Research*, *110*, B03201. https://doi.org/10.1029/2004JB003102

Vezzoli, L. (1988). Island of Ischia. Quaderni de 'La Ricerca Scientifica'. *Consiglio Nazionale Ricerche Roma*, *114*(10), 7–126.

Wassermann, J. (2002). Volcano seismology. In P. Bormann (Ed.), *IASPEI New Manual of Seismological Observatory Practice* (Vol. 1, p. 42). GeoForschungsZentrum, Potsdam.

Yague-Martinez, N., Prats-Iraola, P., Rodriguez Gonzalez, F., Brcic, R., Shau, R., Geudtner, D., et al. (2016). Interferometric processing of Sentinel-1 TOPS data. *IEEE Transactions on Geoscience and Remote Sensing*, *54*(4), 2220–2234. https://doi.org/10.1109/TGRS.2015.2497902

Zhu, L. (2003). Recovering permanent displacements from seismic records of the June 9, 1994 Bolivia deep earthquake. *Geophysical Research Letters*, *30*(14), 1740. https://doi.org/10.1029/2003GL017302

Zobin, V. M. (2003). *Introduction to volcanic seismology* (pp. 474). Amsterdam, New York, Tokyo: Elsevier.

Zollo, A., Judenherc, S., Auger, E., D'Auria, L., Virieux, J., Capuano, P., et al. (2003). Evidence for the buried rim of Campi Flegrei caldera from 3-d active seismic imaging. *Geophysical Research Letters*, *30*(19), 2002. https://doi.org/10.1029/2003GL018173